The imaging equation for a microgrid linear Stokes polarimeter

Israel J. Vaughn

Advanced Sensing Lab, College of Optical Sciences, University of Arizona, USA

ABSTRACT

Imaging polarimeters have currently and historically been largely used for remote sensing tasks. They have also been used to evaluate the defects and calibrate the polarization of liquid crystal displays. A particular type of polarimeter that has a great deal of unrealized potential is the microgrid array linear Stokes polarimeter. This type of polarimeter is not often used because of reconstruction errors. If these errors could be minimized, or mitigated via proper algorithmic reconstruction, then they have advantages over other types of polarimeters, mainly calibration (not much is needed) and proper operation over wide wavelength bands (due to the use of wire grid linear polarizers). In the paper I analyze the imaging equation of the microgrid Stokes polarimeter, using the full vectorial electric field.

1. INTRODUCTION

Imaging polarimeters have proven to be powerful tools for a wide variety of remote sensing tasks. Active and passive polarimeters for remote sensing have been developed for usage in many regions of the optical spectrum. Polarimeters have been used to detect targets with clutter,[1] target identification,[2] penetrate scattering media[2–4] and aid in three-dimensional image reconstruction.[5] Polarimeters have been utilized in atmospheric sensing applications, including determination of aerosol properties,[6] discrimination of ice/water phase particulates in clouds,[7] and observation of plasmas in rocket engine exhaust.[8] Polarimeters have been used to estimate vegetation height, type, and quantity.[9,10] Polarimeters have been also been used in industry to detect defects in and calibrate liquid crystal displays.[11,12]

Historically microgrid Stokes polarimeters have had many issues,[13–16] including pixel registration problems, microgrid polarizer orientation manufacturing issues, aliasing, etc. Recently some advances have been made algorithmically to improve the estimation, given the physical problems with microgrid systems. For example, Tyo *et al*[17] and LaCasse[18] have applied basic sampling theory to improve results with band limited assumptions on either spatial or temporal frequency of the object being imaged. In this paper, I derive the complete imaging operator of a physical microgrid polarimeter system, given certain assumptions.

Please note that capital bold letters denote matrices, while lower case bold letters denote vectors, unless otherwise stated.

2. OVERVIEW OF A MICROGRID STOKES POLARIMETER

The microgrid linear Stokes polarimeter uses a micro array of wire grid linear polarizers placed on top of some kind of focal plane array. A scene is usually imaged using standard imaging optics (lenses) and the linear Stokes information is determined from the irradiance on the detector after passing through the micro array of wire grid polarizers. A schematic is shown in Fig. 1.

Focal plane arrays (FPA) are typically charge coupled devices (CCD) or complementary metal oxide semiconductor (CMOS) for the visible spectrum, and usually indium gallium arsenide (InGaAs) for the near infrared (NIR) spectrum. The microgrid array is then attached onto the front side of the FPA. A schematic of a typical array is shown in Fig. 2(a). The wire grids are typically arranged in an alternating pattern, the first row will alternate between a square wire grid polarizer oriented at 0° and a square wire grid polarizer oriented at 45°, then the next row will alternate between a square (or rectangular) wire grid polarizer oriented at 90° and a

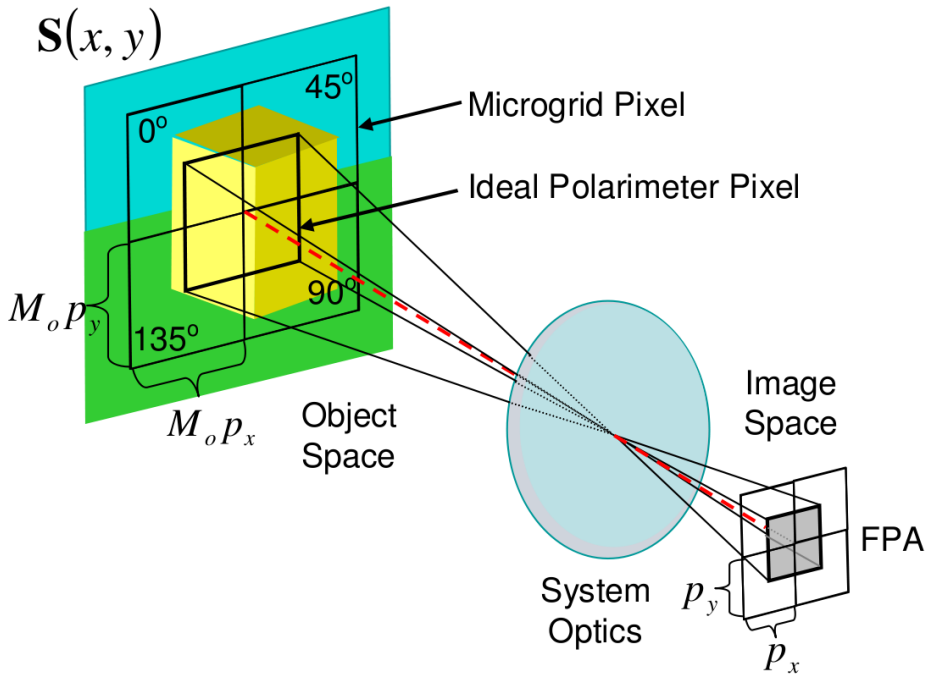

Figure 1. Schematic of a microgrid array Stokes polarimeter. (Courtesy of Ratliff *et al*[15])

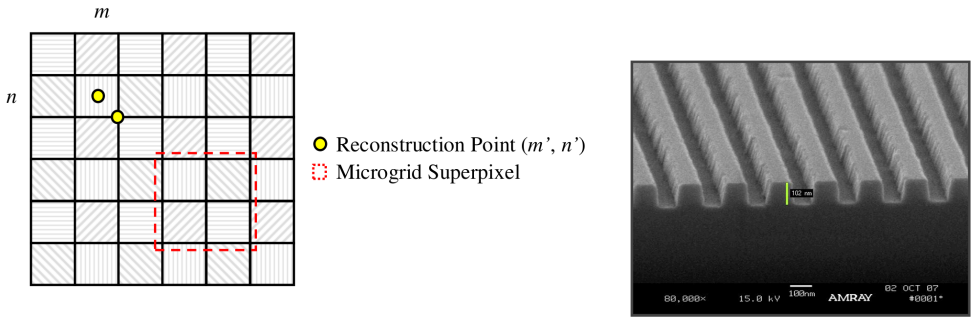

(a) Microgrid Schematic (b) Lithographic microgrid

Figure 2. Schematic of a microgrid array (a) (Courtesy of Ratliff *et al*[15]), alternating rows have the elements oriented at 0°, 45° and 90°, 135° respectively. (b) shows a lithographically manufactured wiregrid (Courtesy of Plymouth Grating).

square wire grid polarizer oriented at 135°, then the next row will be identical to the first row, etc. The size of each wire grid polarizer is determined by the pixel size of the underlying FPA.

For proper function, (i.e. in order to have a polarizer instead of a diffraction grating) the grid spacing must be on the order of, but typically much less than, the wavelength of interest. At optical wavelengths (including NIR) this forces the grid spacing to be extremely small, so lithographic etching techniques are needed to manufacture suitable wire grid linear polarizers. See Fig. 2(b) for an example.

These arrays frequently have manufacturing defects especially in the orientation of the grid. Our lab recently measured orientation errors as much as nearly 11° (although our example is about 17 years old). This can be corrected by inputing a known polarization state of light and measuring the actual pixel values vs. the theoretical pixel values. Effective algorithmic reconstruction of the polarized vector field that is imaged by the polarimeter (usually using the Stokes formalism) is an ongoing area of research.

Further author information: email : ivaughn@optics.arizona.edu
http://www.optics.arizona.edu/asl

The microgrid linear Stokes polarimeter typically uses off the shelf camera optics to image an object or scene onto the microgrid array/FPA device. The optics are usually chosen such that they are (nearly) diffraction limited.

The primary concern when using imaging optics for any polarimeter is that the optics will change the polarization properties of the incident field. In this paper, however, I shall ignore the optical effects of the imaging system, as this has already been analyzed in the literature.[20–22]

3. HOW A WIRE GRID POLARIZER WORKS

A linear wire grid polarizer is often intuitively described for a plane wave in the following way; if the plane wave is polarized parallel to the wires, then the wires are long enough that a current can be induced (electrons excited), which acts like a "mirror", which reflects the plane wave. If the plane wave is perpendicular to the wires, then the wires are so thin that there is almost no current induced, and the wires appear to be transparent. See Fig. 3 Since any oriented plane wave has parallel and perpendicular components, both perpendicular to the propagation direction in free space, the polarizer only passes the component perpendicular to the wires. As long as the wire spacing is small compared with the wavelength, the device acts like a polarizer and not a diffraction grating. This gives the wire grid polarizer the advantage of acting as a polarizer for large acceptance angles, and more importantly large spectral bandwidths.

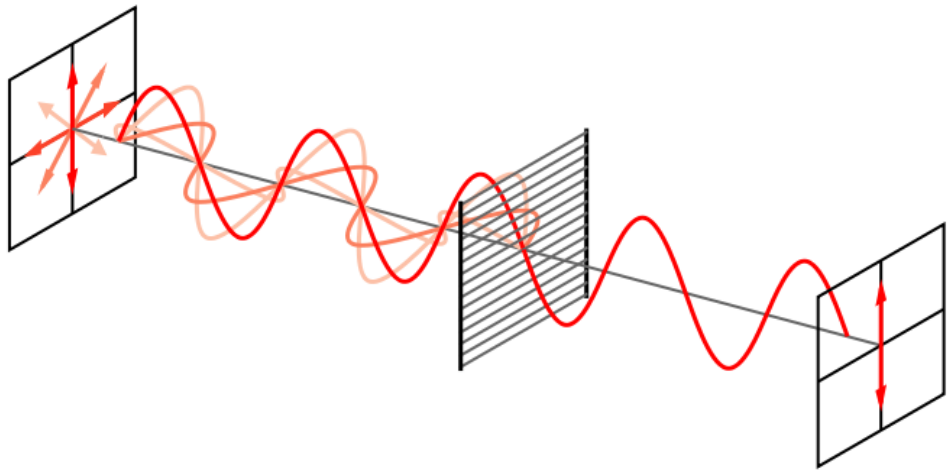

Figure 3. Wire grid polarizer and incident plane waves of various polarizations. (Courtesy of Wikipedia Commons)

4. PROPAGATION THROUGH A SINGLE IDEAL LINEAR WIRE GRID POLARIZER AND INCIDENT ON A SINGLE PIXEL

In this section I investigate the electric field operator from an input field just before the wire grid polarizer to the pixel. This corresponds to the operator acting on what ever electric field is actually imaged to the FPA, per pixel.

In general the following equation describes an imaging system,

$$\mathbf{g}(\mathbf{r},t) = \mathcal{H}\mathbf{f}(\mathbf{r},t) + \mathbf{n}, \quad \mathbf{f} \in \mathbb{C}^3,\ \mathbf{g} \in \mathbb{C}^3,\ \mathbf{n} \in \mathbb{C}^3,\ \mathbf{r} \in \mathbb{R}^3,\ t \in \mathbb{R} \tag{4.1}$$

where $\mathbf{f}(\mathbf{r},t)$ is the full vector electric field (using the complex representation) of electromagnetic radiation exiting our object, $\mathcal{H}$ describes an operator that changes the vector field in some way, and $\mathbf{g}(\mathbf{r},t)$ is the full vector field after the operator. Of course, the real part must be taken to obtain the physical quantities. $\mathcal{H}$ corresponds to a series of polarization elements, while the exiting $\mathbf{g}(\mathbf{r},t)$ will be measured on a detector which collapses the electric vector field to a scalar irradiance measurement. This must be done multiple times, changing $\mathcal{H}$ for each measurement in order to reconstruct the original vector field.

4.1 Poynting vector and plane waves

Any vector field whose components are elements of a separable Hilbert space can be represented as a possibly infinite but countable superposition of plane waves,[30] so $\mathbf{f}$ can represented as

$$\sum_j \mathbf{e}_j \exp\left[i\left(\mathbf{k}_j \cdot \mathbf{r} - \omega_j t\right)\right] \tag{4.2}$$

where the $\mathbf{e}_j = (E_{j_1}, E_{j_2}, E_{j_3})$ are possibly complex field amplitudes. The sum can be reordered since it is countable and uniformly convergent (if it wasn't then an arbitrary field couldn't be represented as a superposition of plane waves, this restricts the forms the sum can take mathematically). In this specific case, it can be assumed that $\mathbf{f}$ is statistically stationary in time, given constant illumination of an object. For example, in a sunlight scene, typically the sun position with respect to the observed object is moving very slowly compared with acquisition time, and the light illuminating the object being imaged has undergone multiple scattering events, which can be modeled using stochastic processes. If $\mathbf{n}$ is AWGN, then it too is statistically stationary, which implies that $\mathbf{g}$ is stationary. To model the measurement of $\mathbf{g}$ the Poynting vector is used;

$$\mathbf{s}(\mathbf{r}, t) = \mathrm{Re}\left[\mathbf{e}(\mathbf{r}, t)\right] \times \mathrm{Re}\left[\mathbf{h}(\mathbf{r}, t)\right] \tag{4.3}$$

where $\times$ denotes the cross product, $\mathbf{e}$ is the complex electric field, and $\mathbf{h}$ is the complex magnetic (induction) field. It can be shown that the time average of a Poynting vector for an electromagnetic plane wave in a homogeneous, isotropic, linear medium, i.e.

$$\begin{aligned} \text{Electric vector field} &= \mathrm{Re}[\mathbf{e}_0 e^{i(\mathbf{k}\cdot\mathbf{r}-\omega t)}] \\ \text{Magnetic vector field} &= \mathrm{Re}[\mathbf{h}_0 e^{i(\mathbf{k}\cdot\mathbf{r}-\omega t)}], \end{aligned} \tag{4.4}$$

where $\mathbf{e}_0 = \mathbf{e}_0^{'} + i\mathbf{e}_0^{''}$ is the possibly complex electric amplitude, $\mathbf{h}_0 = \mathbf{h}_0^{'} + i\mathbf{h}_0^{''}$ is the possibly complex magnetic amplitude, and $\mathbf{k} = \mathbf{k}^{'} + i\mathbf{k}^{''}$ is the possibly complex wave vector; can be represented in the following form :

$$\langle \mathbf{s}(\mathbf{r}) \rangle_t = \frac{e^{-2\mathbf{k}''\cdot\mathbf{r}}}{2} \frac{\left(\|\mathbf{e}_0^{'}\|^2 + \|\mathbf{e}_0^{''}\|^2\right)(\mu'\mathbf{k}' + \mu''\mathbf{k}'') - 2(\mu'\mathbf{k}'' - \mu''\mathbf{k}') \times (\mathbf{e}_0^{'} \times \mathbf{e}_0^{''})}{z_0(\omega/c)(\mu'^2 + \mu''^2)}. \tag{4.5}$$

$\mu(\omega) = \mu^{'}(\omega) + i\mu^{''}(\omega) = 1 + \chi_m(\omega)$ is the complex magnetic permeability and z_0 is the impedance of free space. This assumes that $\mathbf{s}(\mathbf{r}, t)$ is statistically stationary. Note that the $\times$ symbols in the above equation denote cross products. If the plane wave is in a typical optical medium then $\mathrm{Im}[\epsilon(\omega)] \approx 0$ and $\mathrm{Im}[\mu(\omega)] \approx 0$. Additionally if $\mathbf{k}'' = 0$ then Eqn. 4.5 can be simplified to

$$\langle \mathbf{s}(\mathbf{r}) \rangle_t = \frac{1}{2} \frac{\left(\|\mathbf{e}_0^{'}\|^2 + \|\mathbf{e}_0^{''}\|^2\right)}{z_0\sqrt{\mu(\omega)/\epsilon(\omega)}} \hat{\mathbf{k}} \tag{4.6}$$

where $\hat{\mathbf{k}} = \mathbf{k}/\|\mathbf{k}\|$. The irradiance at a single point, $\mathbf{r}$, is usually defined as the time average of the Poynting vector.

Equation 4.6 is for a single plane wave, so I must generalize the equation for an arbitrary superposition of plane waves. For an arbitrary superposition of plane waves

$$\mathbf{s}(\mathbf{r}, t) = \mathrm{Re}\left(\sum_j \mathbf{e}_j \exp\left[i\left(\mathbf{k}_j \cdot \mathbf{r} - \omega_j t\right)\right]\right) \times \mathrm{Re}\left(\sum_j \mathbf{h}_j \exp\left[i\left(\mathbf{k}_j \cdot \mathbf{r} - \omega_j t\right)\right]\right). \tag{4.7}$$

Since

$$\mathrm{Re}(z) = \frac{1}{2}\left(z + z^*\right) \tag{4.8}$$

where $*$ denotes the complex conjugate Eqn. 4.7 can be rewritten

$$\mathbf{s}(\mathbf{r},t) = \frac{1}{4}\sum_j\sum_{j'}\begin{pmatrix} & \mathbf{e}_j \times \mathbf{h}_{j'} \exp\left[i(\mathbf{k}_j + \mathbf{k}_{j'})\cdot\mathbf{r} - i(\omega_j + \omega_{j'})t\right] \\ + & \mathbf{e}_j \times \mathbf{h}^*_{j'} \exp\left[i(\mathbf{k}_j - \mathbf{k}_{j'})\cdot\mathbf{r} - i(\omega_j - \omega_{j'})t\right] \\ + & \mathbf{e}^*_j \times \mathbf{h}_{j'} \exp\left[-i(\mathbf{k}_j - \mathbf{k}_{j'})\cdot\mathbf{r} + i(\omega_j - \omega_{j'})t\right] \\ + & \mathbf{e}^*_j \times \mathbf{h}^*_{j'} \exp\left[-i(\mathbf{k}_j + \mathbf{k}_{j'})\cdot\mathbf{r} + i(\omega_j + \omega_{j'})t\right] \end{pmatrix} \tag{4.9}$$

In the above equation the terms inside the parentheses are added because the equation will not fit on a single line, the parentheses do not represent a vector. When $j = j'$ the time average of $\mathbf{s}$ for that portion of the sum is the same as in Eqn. 4.5. What about when $j \neq j'$? Then the electric field is not associated with the magnetic field, and hence the cross product is not perpendicular to either plane wave. The time average can be taken inside the sum and then the following four integrals must be evaluated :

$$\lim_{T\to\infty}\frac{1}{2T}\int_{-T}^{T}\exp\left[-i(\omega_j + \omega_{j'})t\right]dt \tag{4.10a}$$

$$\lim_{T\to\infty}\frac{1}{2T}\int_{-T}^{T}\exp\left[-i(\omega_j - \omega_{j'})t\right]dt \tag{4.10b}$$

$$\lim_{T\to\infty}\frac{1}{2T}\int_{-T}^{T}\exp\left[i(\omega_j - \omega_{j'})t\right]dt \tag{4.10c}$$

$$\lim_{T\to\infty}\frac{1}{2T}\int_{-T}^{T}\exp\left[i(\omega_j + \omega_{j'})t\right]dt \tag{4.10d}$$

Since they are sinusoids, they average to zero in all except the following special cases :

$$\omega_j = \omega_{j'}, \tag{4.11a}$$

$$\omega_j = -\omega_{j'}. \tag{4.11b}$$

From Maxwell's equations, each plane wave component has the following property

$$\mathbf{k}_j\cdot\mathbf{k}_j = \mathbf{k}'_j\cdot\mathbf{k}'_j - \mathbf{k}''_j\cdot\mathbf{k}''_j + 2i\mathbf{k}'_j\cdot\mathbf{k}''_j = \omega_j^2\epsilon_0\mu_0\epsilon(\omega_j)\mu(\omega_j) = \left(\frac{\omega_j}{c}\right)^2\epsilon(\omega_j)\mu(\omega_j) \tag{4.12}$$

but after the polarizer elements which constitute $\mathcal{H}$ the field is usually propagating in air, which is close enough to free space such that $\epsilon(\omega_j) = \mu(\omega_j) \approx 1$. This implies there is no imaginary component of the equation so

$$\mathbf{k}_j\cdot\mathbf{k}_j = \mathbf{k}'_j\cdot\mathbf{k}'_j = \left(\frac{\omega_j}{c}\right)^2 \tag{4.13}$$

If $\omega_j = \omega_{j'}$ then

$$\lim_{T\to\infty}\frac{1}{2T}\int_{-T}^{T}\exp\left[-i(\omega_j + \omega_{j'})t\right]dt = 0 \tag{4.14a}$$

$$\lim_{T\to\infty}\frac{1}{2T}\int_{-T}^{T}\exp\left[-i(\omega_j - \omega_{j'})t\right]dt = 1 \tag{4.14b}$$

$$\lim_{T\to\infty}\frac{1}{2T}\int_{-T}^{T}\exp\left[i(\omega_j - \omega_{j'})t\right]dt = 1 \tag{4.14c}$$

$$\lim_{T\to\infty}\frac{1}{2T}\int_{-T}^{T}\exp\left[i(\omega_j + \omega_{j'})t\right]dt = 0 \tag{4.14d}$$

and if $\omega_j = -\omega_{j'}$ then

$$\lim_{T\to\infty} \frac{1}{2T} \int_{-T}^{T} \exp\left[-i(\omega_j + \omega_{j'})t\right] dt = 1 \tag{4.14e}$$

$$\lim_{T\to\infty} \frac{1}{2T} \int_{-T}^{T} \exp\left[-i(\omega_j - \omega_{j'})t\right] dt = 0 \tag{4.14f}$$

$$\lim_{T\to\infty} \frac{1}{2T} \int_{-T}^{T} \exp\left[i(\omega_j - \omega_{j'})t\right] dt = 0 \tag{4.14g}$$

$$\lim_{T\to\infty} \frac{1}{2T} \int_{-T}^{T} \exp\left[i(\omega_j + \omega_{j'})t\right] dt = 1. \tag{4.14h}$$

This implies that

$$\begin{aligned}
\langle \mathbf{s}(\mathbf{r},t)\rangle_t &= \frac{1}{4}\sum_j \sum_{j'} \begin{pmatrix} & \mathbf{e}_j \times \mathbf{h}_{j'} \exp\left(i(\mathbf{k}_j + \mathbf{k}_{j'})\cdot \mathbf{r}\right) \\ + & \mathbf{e}_j \times \mathbf{h}^*_{j'} \exp\left(i(\mathbf{k}_j - \mathbf{k}_{j'})\cdot \mathbf{r}\right) \\ + & \mathbf{e}^*_j \times \mathbf{h}_{j'} \exp\left(-i(\mathbf{k}_j - \mathbf{k}_{j'})\cdot \mathbf{r}\right) \\ + & \mathbf{e}^*_j \times \mathbf{h}^*_{j'} \exp\left(-i(\mathbf{k}_j + \mathbf{k}_{j'})\cdot \mathbf{r}\right) \end{pmatrix} \\
&= \frac{1}{4}\sum_j \sum_{j'} \begin{pmatrix} & 2\,\mathrm{Re}\left[\mathbf{e}_j \times \mathbf{h}_{j'} \exp\left(i(\mathbf{k}_j + \mathbf{k}_{j'})\cdot \mathbf{r}\right)\right] \\ \\ + & 2\,\mathrm{Re}\left[\mathbf{e}_j \times \mathbf{h}^*_{j'} \exp\left(i(\mathbf{k}_j - \mathbf{k}_{j'})\cdot \mathbf{r}\right)\right] \end{pmatrix}
\end{aligned} \tag{4.15}$$

where the j' indices are restricted to only those where $\omega_j = \omega_{j'}$ or $\omega_j = -\omega_{j'}$ for each fixed j. Eqn. 4.13 also forces the following condition :

$$\|\mathbf{k}_j\|^2 = \|\mathbf{k}_{j'}\|^2 \tag{4.16}$$

This means that any corresponding $\mathbf{k}_{j'}$ vector must lie on the sphere of radius $\|\mathbf{k}_j\|$.

4.2 Polarization components and the vector field

The polarization change can be explicitly computed using material properties, but $\mathcal{H}$ is used instead to describe the change of the vector field through a polarization component. In the complex plane wave representation that is being used, the real and imaginary parts of $\mathbf{e}_j$, along with the real parts of the exponential, define the polarization properties. Explicitly

$$\begin{aligned}
\mathbf{e}(\mathbf{r},t) &= \mathrm{Re}\left[\mathbf{e}_0 e^{\mathbf{k}\cdot\mathbf{r}-\omega t}\right] \\
&= e^{-\mathbf{k}''\cdot\mathbf{r}}\,\mathrm{Re}\left[(\mathbf{e}'_0 + i\mathbf{e}''_0)e^{i(\mathbf{k}'\cdot\mathbf{r}-\omega t)}\right] \\
&= e^{-\mathbf{k}''\cdot\mathbf{r}}\left[\mathbf{e}'_0\cos(\mathbf{k}'\cdot\mathbf{r}-\omega t) - \mathbf{e}''_0\sin(\mathbf{k}'\cdot\mathbf{r}-\omega t)\right]
\end{aligned} \tag{4.17}$$

Since the plane waves before the polarizer elements are propagating in air, $\mathbf{k}'' \approx 0$. So $\mathcal{H}$ acts on

$$\boxed{\mathbf{e}(\mathbf{r},t) = \left[e'_0\cos(\mathbf{k}'\cdot\mathbf{r}-\omega t)\right]\hat{\mathbf{e}}'_0 - \left[e''_0\sin(\mathbf{k}'\cdot\mathbf{r}-\omega t)\right]\hat{\mathbf{e}}''_0} \tag{4.18}$$

where $\hat{\mathbf{e}}'_0, \hat{\mathbf{e}}''_0$ are unit vectors.

Ideally, the polarizer transmission does not depend on the amplitude terms (the sine and cosine terms inside the brackets) in Eqn. 4.18, so only the vector terms matter. The polarizer must be oriented in space, so the coordinates can be chosen. For this analysis, it is assumed that the polarizer can be modeled as a plane element, with normal pointing in the $\hat{\mathbf{z}}$ direction. In reality, wire grid linear polarizers work well for a range of angles less than $\pm\pi/2$ with respect to $\hat{\mathbf{z}}$. The physics change as the angle becomes large due to Brewster's angle (of the substrate) and other effects,[23] these details will not be included here. This analysis assumes that the polarizer

is ideal over the entire range of angles $(-\pi/2, \pi/2]$ and that it is large with respect to the angular subtense of the electric field being measured. The polarizer will be defined to have the transmission axis at angle θ with respect to the positive x-axis. If the polarizer is thin, just like the wires, and/or on a dielectric substrate, then only reflection of the plane waves affect the transmission of the z components, this is partially responsible for the polarizer performance as a function of angle with respect to $\hat{\mathbf{z}}$.

The components of each plane wave must first be projected onto the xy-plane :

$$\mathbf{e}'_{\text{proj}} = \mathbf{e}' - (\mathbf{e}' \cdot \hat{\mathbf{z}})\hat{\mathbf{z}} \tag{4.19a}$$

$$\mathbf{e}''_{\text{proj}} = \mathbf{e}'' - (\mathbf{e}'' \cdot \hat{\mathbf{z}})\hat{\mathbf{z}} \tag{4.19b}$$

i.e. first each component is projected onto the normal, $\hat{\mathbf{z}}$, then subtracted that projection to get the component on the xy-plane. Then only the components oriented in the θ or $-\theta$ direction are transmitted, i.e.

$$\mathbf{e}'_{\text{trans,xy}} = \left[\mathbf{e}'_{\text{proj}} \cdot \begin{pmatrix}\cos\theta \\ \sin\theta \\ 0\end{pmatrix}\right] \begin{pmatrix}\cos\theta \\ \sin\theta \\ 0\end{pmatrix} \tag{4.20a}$$

$$\mathbf{e}''_{\text{trans,xy}} = \left[\mathbf{e}''_{\text{proj}} \cdot \begin{pmatrix}\cos\theta \\ \sin\theta \\ 0\end{pmatrix}\right] \begin{pmatrix}\cos\theta \\ \sin\theta \\ 0\end{pmatrix} \tag{4.20b}$$

The above determines the x, y components of both $\mathbf{e}', \mathbf{e}''$, with the direction of the z components direction assumed to be unchanged (at least outside of the near field), note that to satisfy Maxwell's equations the z components amplitude may change, but as shown later the z components disappear so this calculation is not analyzed here. Simplifying the equation above results in

$$\mathbf{e}'_{\text{trans}} = \begin{pmatrix}(e'_x \cos\theta + e'_y \sin\theta)\cos\theta \\ (e'_x \cos\theta + e'_y \sin\theta)\sin\theta \\ e'_z\end{pmatrix} \tag{4.21a}$$

$$\mathbf{e}''_{\text{trans}} = \begin{pmatrix}(e''_x \cos\theta + e''_y \sin\theta)\cos\theta \\ (e''_x \cos\theta + e''_y \sin\theta)\sin\theta \\ e''_z\end{pmatrix} \tag{4.21b}$$

for a single plane wave. As a consequence of the superposition principle the total field is

$$\begin{aligned}\mathbf{e}_{\text{trans}} &= \sum_j \left[\begin{pmatrix}(e'_{x,j} \cos\theta + e'_{y,j} \sin\theta)\cos\theta \\ (e'_{x,j} \cos\theta + e'_{y,j} \sin\theta)\sin\theta \\ e'_{z,j}\end{pmatrix} \cos(\mathbf{k}'_j \cdot \mathbf{r} - \omega_j t)\right. \\ &\quad \left. - \begin{pmatrix}(e''_{x,j} \cos\theta + e''_{y,j} \sin\theta)\cos\theta \\ (e''_{x,j} \cos\theta + e''_{y,j} \sin\theta)\sin\theta \\ e''_{z,j}\end{pmatrix} \sin(\mathbf{k}'_j \cdot \mathbf{r} - \omega_j t)\right] \\ &= \sum_j \text{Re}\left\{\left[\begin{pmatrix}(e'_{x,j} \cos\theta + e'_{y,j} \sin\theta)\cos\theta \\ (e'_{x,j} \cos\theta + e'_{y,j} \sin\theta)\sin\theta \\ e'_{z,j}\end{pmatrix} + i \begin{pmatrix}(e''_{x,j} \cos\theta + e''_{y,j} \sin\theta)\cos\theta \\ (e''_{x,j} \cos\theta + e''_{y,j} \sin\theta)\sin\theta \\ e''_{z,j}\end{pmatrix}\right] e^{\mathbf{k}'_j \cdot \mathbf{r} - \omega_j t}\right\}. \end{aligned} \tag{4.22}$$

This implies that

$$\mathcal{H}(\theta) = \begin{pmatrix}\cos^2\theta & \cos\theta\sin\theta & 0 \\ \cos\theta\sin\theta & \sin^2\theta & 0 \\ 0 & 0 & 1\end{pmatrix}. \tag{4.23}$$

Notice that $\mathcal{H}$ is self-adjoint. The propagating electric field is still a superposition of plane waves in basically free space, so from Maxwell's equations the $\mathbf{h}_j$ vectors are mutually perpendicular to both $\mathbf{e}_j$ and $\mathbf{k}'_j$. From Maxwell's equations it can be easily shown that

$$\mathbf{h} = \frac{1}{\mu_0 \omega}\mathbf{k}' \times \mathbf{e} \tag{4.24}$$

for each plane wave. The irradiance measured on the detector from Eqns. 4.15, 4.24 is then

$$\langle \mathbf{s}(\mathbf{r},t)\rangle_t = \frac{1}{4}\sum_j\sum_{j'}\frac{1}{\mu_0\omega_{j'}}\begin{pmatrix} \left[(\mathcal{H}\mathbf{e}_j\cdot\mathcal{H}\mathbf{e}_{j'})\mathbf{k}_{j'} - (\mathcal{H}\mathbf{e}_j\cdot\mathbf{k}_{j'})\mathcal{H}\mathbf{e}_{j'}\right]\exp\left(i(\mathbf{k}_j+\mathbf{k}_{j'})\cdot\mathbf{r}\right) \\ + \quad \left[(\mathcal{H}\mathbf{e}_j\cdot\mathcal{H}\mathbf{e}^*_{j'})\mathbf{k}_{j'} - (\mathcal{H}\mathbf{e}_j\cdot\mathbf{k}_{j'})\mathcal{H}\mathbf{e}^*_{j'}\right]\exp\left(i(\mathbf{k}_j-\mathbf{k}_{j'})\cdot\mathbf{r}\right) \\ + \quad \left[(\mathcal{H}\mathbf{e}^*_j\cdot\mathcal{H}\mathbf{e}_{j'})\mathbf{k}_{j'} - (\mathcal{H}\mathbf{e}^*_j\cdot\mathbf{k}_{j'})\mathcal{H}\mathbf{e}_{j'}\right]\exp\left(-i(\mathbf{k}_j-\mathbf{k}_{j'})\cdot\mathbf{r}\right) \\ + \quad \left[(\mathcal{H}\mathbf{e}^*_j\cdot\mathcal{H}\mathbf{e}^*_{j'})\mathbf{k}_{j'} - (\mathcal{H}\mathbf{e}^*_j\cdot\mathbf{k}_{j'})\mathcal{H}\mathbf{e}^*_{j'}\right]\exp\left(-i(\mathbf{k}_j+\mathbf{k}_{j'})\cdot\mathbf{r}\right) \end{pmatrix} \tag{4.25}$$

by using the vector identity

$$\mathbf{a}\times(\mathbf{b}\times\mathbf{c}) = (\mathbf{a}\cdot\mathbf{c})\mathbf{b} - (\mathbf{a}\cdot\mathbf{b})\mathbf{c}. \tag{4.26}$$

Note that since the plane waves are in air, $\mathbf{k}_j = \mathbf{k}'_j$ and $\mathbf{k}_{j'} = \mathbf{k}'_{j'}$, i.e. all $\mathbf{k}$ vectors are purely real.

Now each component from Eqn. 4.22 can be substituted into Eqn. 4.25. First the inner products in front of the $\mathbf{k}$ vector terms are computed.

$$(\mathcal{H}\mathbf{e}_j\cdot\mathcal{H}\mathbf{e}_{j'})\mathbf{k}_{j'} = [(\mathcal{H}^2\mathbf{e}_j)\cdot\mathbf{e}_{j'}]\mathbf{k}_{j'}, \text{ since } \mathcal{H} \text{ is self-adjoint} \tag{4.27}$$

where

$$\mathcal{H}^2(\theta) = \begin{pmatrix} \cos^4\theta+\cos^2\theta\sin^2\theta & \cos^3\theta\sin\theta+\cos\theta\sin^3\theta & 0 \\ \cos^3\theta\sin\theta+\cos\theta\sin^3\theta & \sin^4\theta+\cos^2\theta\sin^2\theta & 0 \\ 0 & 0 & 1 \end{pmatrix}. \tag{4.28}$$

Additionally

$$\begin{aligned}(\mathcal{H}^2\mathbf{e}_j\cdot\mathbf{e}_{j'})\mathbf{k}_{j'} &= [(\mathcal{H}^2\mathbf{e}'_j + i\mathcal{H}^2\mathbf{e}'')\cdot(\mathbf{e}'_{j'}+i\mathbf{e}''_{j'})]\mathbf{k}_{j'} \\ &= [\mathcal{H}^2\mathbf{e}'_j\cdot\mathbf{e}'_{j'} + i\mathcal{H}^2\mathbf{e}'_j\cdot\mathbf{e}''_{j'} + i\mathcal{H}^2\mathbf{e}''_j\cdot\mathbf{e}'_{j'} - \mathcal{H}^2\mathbf{e}'_j\cdot\mathbf{e}''_{j'}]\mathbf{k}_{j'}.\end{aligned} \tag{4.29a}$$

Similarly

$$(\mathcal{H}^2\mathbf{e}_j\cdot\mathbf{e}^*_{j'})\mathbf{k}_{j'} = [\mathcal{H}^2\mathbf{e}'_j\cdot\mathbf{e}'_{j'} + i\mathcal{H}^2\mathbf{e}'_j\cdot\mathbf{e}''_{j'} - i\mathcal{H}^2\mathbf{e}''_j\cdot\mathbf{e}'_{j'} + \mathcal{H}^2\mathbf{e}'_j\cdot\mathbf{e}''_{j'}]\mathbf{k}_{j'} \tag{4.29b}$$

$$(\mathcal{H}^2\mathbf{e}^*_j\cdot\mathbf{e}_{j'})\mathbf{k}_{j'} = [\mathcal{H}^2\mathbf{e}'_j\cdot\mathbf{e}'_{j'} - i\mathcal{H}^2\mathbf{e}'_j\cdot\mathbf{e}''_{j'} + i\mathcal{H}^2\mathbf{e}''_j\cdot\mathbf{e}'_{j'} + \mathcal{H}^2\mathbf{e}'_j\cdot\mathbf{e}''_{j'}]\mathbf{k}_{j'} \tag{4.29c}$$

$$(\mathcal{H}^2\mathbf{e}^*_j\cdot\mathbf{e}^*_{j'})\mathbf{k}_{j'} = [\mathcal{H}^2\mathbf{e}'_j\cdot\mathbf{e}'_{j'} - i\mathcal{H}^2\mathbf{e}'_j\cdot\mathbf{e}''_{j'} - i\mathcal{H}^2\mathbf{e}''_j\cdot\mathbf{e}'_{j'} - \mathcal{H}^2\mathbf{e}'_j\cdot\mathbf{e}''_{j'}]\mathbf{k}_{j'} \tag{4.29d}$$

and explicitly

$$
\begin{aligned}
(\mathcal{H}^2\mathbf{e}_j\cdot\mathbf{e}_{j'})\mathbf{k}_{j'} = \Big[& e'_{x,j}e'_{x,j'}\cos^4\theta + (e'_{x,j}e'_{y,j'}+e'_{x,j'}e'_{y,j})\cos^3\theta\sin\theta + e'_{y,j}e'_{y,j'}\cos^2\theta\sin^2\theta \\
& + e'_{x,j}e'_{x,j'}\cos^2\theta\sin^2\theta + (e'_{x,j}e'_{y,j'}+e'_{x,j'}e'_{y,j})\sin^3\theta\cos\theta + e'_{y,j}e'_{y,j'}\sin^4\theta \\
& + e'_{z,j}e'_{y,j'} \\
& - e''_{x,j}e''_{x,j'}\cos^4\theta - (e''_{x,j}e''_{y,j'}-e''_{x,j'}e''_{y,j})\cos^3\theta\sin\theta + e''_{y,j}e''_{y,j'}\cos^2\theta\sin^2\theta \\
& - e''_{x,j}e''_{x,j'}\cos^2\theta\sin^2\theta - (e''_{x,j}e''_{y,j'}-e''_{x,j'}e''_{y,j})\sin^3\theta\cos\theta - e''_{y,j}e''_{y,j'}\sin^4\theta \\
& - e''_{z,j}e''_{y,j'} \\
& + i\Big(e''_{x,j}e'_{x,j'}\cos^4\theta + (e''_{x,j}e'_{y,j'}+e'_{x,j'}e''_{y,j})\cos^3\theta\sin\theta + e''_{y,j}e'_{y,j'}\cos^2\theta\sin^2\theta \\
& + e''_{x,j}e'_{x,j'}\cos^2\theta\sin^2\theta + (e''_{x,j}e'_{y,j'}+e'_{x,j'}e''_{y,j})\sin^3\theta\cos\theta + e''_{y,j}e'_{y,j'}\sin^4\theta \\
& + e''_{z,j}e'_{y,j'} \\
& + e'_{x,j}e''_{x,j'}\cos^4\theta + (e'_{x,j}e''_{y,j'}+e''_{x,j'}e'_{y,j})\cos^3\theta\sin\theta + e'_{y,j}e''_{y,j'}\cos^2\theta\sin^2\theta \\
& + e'_{x,j}e''_{x,j'}\cos^2\theta\sin^2\theta + (e'_{x,j}e''_{y,j'}+e''_{x,j'}e'_{y,j})\sin^3\theta\cos\theta + e'_{y,j}e''_{y,j'}\sin^4\theta \\
& + e'_{z,j}e''_{y,j'}\Big)\Big].
\end{aligned} \tag{4.30}
$$

With similar equations for the other components. The above equation is tedious to manipulate. The detector not only integrates over time, but also over some finite area. If the polarizer is set at $z = 0$ and centered on $(0,0)$ in the xy-plane then the detector is some fixed distance z_0 from the polarizer also centered on $(0,0)$ in the xy-plane. The detector will be assumed to be square here, with side length ℓ. Then

$$
\begin{aligned}
\text{irradiance on detector} &= \int_{-\ell/2}^{\ell/2}\int_{-\ell/2}^{\ell/2}\langle\mathbf{s}(\mathbf{r},t)\rangle_t dxdy \\
&= \int_{-\infty}^{\infty}\int_{-\infty}^{\infty}\text{rect}\left(\frac{x}{\ell},\frac{y}{\ell}\right)\langle\mathbf{s}(\mathbf{r},t)\rangle_t dxdy.
\end{aligned} \tag{4.31}
$$

This integral can be taken inside Eqn. 4.25 and only operates on the exponential terms. The following four integrals are obtained :

$$
e^{i(k_{z,j}+k_{z,j'})z_0}\int_{-\infty}^{\infty}\int_{-\infty}^{\infty}\text{rect}\left(\frac{x}{\ell},\frac{y}{\ell}\right)\exp\big[i(k_{x,j}+k_{x,j'})x + i(k_{y,j}+k_{y,j'})y\big]dxdy \tag{4.32a}
$$

$$
e^{i(k_{z,j}-k_{z,j'})z_0}\int_{-\infty}^{\infty}\int_{-\infty}^{\infty}\text{rect}\left(\frac{x}{\ell},\frac{y}{\ell}\right)\exp\big[i(k_{x,j}-k_{x,j'})x + i(k_{y,j}-k_{y,j'})y\big]dxdy \tag{4.32b}
$$

$$
e^{-i(k_{z,j}-k_{z,j'})z_0}\int_{-\infty}^{\infty}\int_{-\infty}^{\infty}\text{rect}\left(\frac{x}{\ell},\frac{y}{\ell}\right)\exp\big[-i(k_{x,j}-k_{x,j'})x - i(k_{y,j}-k_{y,j'})y\big]dxdy \tag{4.32c}
$$

$$
e^{-i(k_{z,j}+k_{z,j'})z_0}\int_{-\infty}^{\infty}\int_{-\infty}^{\infty}\text{rect}\left(\frac{x}{\ell},\frac{y}{\ell}\right)\exp\big[-i(k_{x,j}+k_{x,j'})x - i(k_{y,j}+k_{y,j'})y\big]dxdy \tag{4.32d}
$$

These all resemble Fourier transforms. These integrals respectively become

$$
\ell^2 e^{i(k_{z,j}+k_{z,j'})z_0}\,\text{sinc}\left(\frac{\ell(k_{x,j}+k_{x,j'})}{2\pi},\frac{\ell(k_{y,j}+k_{y,j'})}{2\pi}\right) \tag{4.33a}
$$

$$
\ell^2 e^{i(k_{z,j}-k_{z,j'})z_0}\,\text{sinc}\left(\frac{\ell(k_{x,j}-k_{x,j'})}{2\pi},\frac{\ell(k_{y,j}-k_{y,j'})}{2\pi}\right) \tag{4.33b}
$$

$$
\ell^2 e^{-i(k_{z,j}-k_{z,j'})z_0}\,\text{sinc}\left(\frac{\ell(-k_{x,j}+k_{x,j'})}{2\pi},\frac{\ell(-k_{y,j}+k_{y,j'})}{2\pi}\right) \tag{4.33c}
$$

$$
\ell^2 e^{-i(k_{z,j}+k_{z,j'})z_0}\,\text{sinc}\left(-\frac{\ell(k_{x,j}+k_{x,j'})}{2\pi},-\frac{\ell(k_{y,j}+k_{y,j'})}{2\pi}\right). \tag{4.33d}
$$

Finally, the vector field irradiance that can possibly be measured by the detector is :

$$\int_{-\ell/2}^{\ell/2}\int_{-\ell/2}^{\ell/2}\langle \mathbf{s}(\mathbf{r},t)\rangle_t dxdy =$$

$$\frac{1}{4}\sum_j\sum_{j'}\frac{\ell^2}{\mu_0\omega_{j'}}\begin{pmatrix} & \Big[(\mathcal{H}\mathbf{e}_j\cdot\mathcal{H}\mathbf{e}_{j'})\mathbf{k}_{j'}-(\mathcal{H}\mathbf{e}_j\cdot\mathbf{k}_{j'})\mathcal{H}\mathbf{e}_{j'}\Big]e^{i(k_{z,j}+k_{z,j'})z_0}\,\mathrm{sinc}\left(\frac{\ell(\boldsymbol{\kappa}_j+\boldsymbol{\kappa}_{j'})}{2\pi}\right) \\ + & \Big[(\mathcal{H}\mathbf{e}_j\cdot\mathcal{H}\mathbf{e}^*_{j'})\mathbf{k}_{j'}-(\mathcal{H}\mathbf{e}_j\cdot\mathbf{k}_{j'})\mathcal{H}\mathbf{e}^*_{j'}\Big]e^{i(k_{z,j}-k_{z,j'})z_0}\,\mathrm{sinc}\left(\frac{\ell(\boldsymbol{\kappa}_j-\boldsymbol{\kappa}_{j'})}{2\pi}\right) \\ + & \Big[(\mathcal{H}\mathbf{e}^*_j\cdot\mathcal{H}\mathbf{e}_{j'})\mathbf{k}_{j'}-(\mathcal{H}\mathbf{e}^*_j\cdot\mathbf{k}_{j'})\mathcal{H}\mathbf{e}_{j'}\Big]e^{-i(k_{z,j}-k_{z,j'})z_0}\,\mathrm{sinc}\left(\frac{\ell(-\boldsymbol{\kappa}_j+\boldsymbol{\kappa}_{j'})}{2\pi}\right) \\ + & \Big[(\mathcal{H}\mathbf{e}^*_j\cdot\mathcal{H}\mathbf{e}^*_{j'})\mathbf{k}_{j'}-(\mathcal{H}\mathbf{e}^*_j\cdot\mathbf{k}_{j'})\mathcal{H}\mathbf{e}^*_{j'}\Big]e^{-i(k_{z,j}+k_{z,j'})z_0}\,\mathrm{sinc}\left(-\frac{\ell(\boldsymbol{\kappa}_j+\boldsymbol{\kappa}_{j'})}{2\pi}\right)\end{pmatrix} \tag{4.34}$$

where

$$\boldsymbol{\kappa} = \begin{pmatrix}k_x\\k_y\end{pmatrix} \tag{4.35}$$

$$\mathrm{sinc}(\boldsymbol{\kappa}) = sinc(k_x,k_y) = \mathrm{sinc}(k_x)\,\mathrm{sinc}(k_y). \tag{4.36}$$

This can be simplified further by attempting to rewrite the plane wave superposition in terms of the original field, and by combining some of the complex terms. Essentially there exists some set of j's for each j satisfying $\|\mathbf{k}_{j'}\| = \|\mathbf{k}_j\|$ and $\omega_{j'} = \pm\omega_j$, and the entire set of js is a representation of the original field, so the equation can be re-indexed in terms of the sets of j's, i.e. for each j' the equation is summed over all js, representing the original field. The complex terms can be simplified :

$$\int_{-\ell/2}^{\ell/2}\int_{-\ell/2}^{\ell/2}\langle \mathbf{s}(\mathbf{r},t)\rangle_t dxdy =$$

$$\sum_j\sum_{j'}\frac{\ell^2}{\mu_0\omega_{j'}}\begin{pmatrix} & \mathrm{Re}\left(\Big[(\mathcal{H}\mathbf{e}_j\cdot\mathcal{H}\mathbf{e}_{j'})\mathbf{k}_{j'}-(\mathcal{H}\mathbf{e}_j\cdot\mathbf{k}_{j'})\mathcal{H}\mathbf{e}_{j'}\Big]e^{i(k_{z,j}+k_{z,j'})z_0}\,\mathrm{sinc}\left(\frac{\ell(\boldsymbol{\kappa}_j+\boldsymbol{\kappa}_{j'})}{2\pi}\right)\right) \\ + & \mathrm{Re}\left(\Big[(\mathcal{H}\mathbf{e}^*_j\cdot\mathcal{H}\mathbf{e}_{j'})\mathbf{k}_{j'}-(\mathcal{H}\mathbf{e}^*_j\cdot\mathbf{k}_{j'})\mathcal{H}\mathbf{e}_{j'}\Big]e^{-i(k_{z,j}-k_{z,j'})z_0}\,\mathrm{sinc}\left(\frac{l(\boldsymbol{\kappa}_j-\boldsymbol{\kappa}_{j'})}{2\pi}\right)\right)\end{pmatrix} \tag{4.37}$$

If it is assumed that the pixels are polarization independent in the measurement of irradiance (not quite true but the polarization sensitivity is low enough that it is a reasonable first order assumption), and that they lie in the x-y plane then the irradiance measured will be the z-component of the Poynting vector. Taking the z-component yields:

$$\boxed{\sum_j\sum_{j'}\frac{\ell^2}{\mu_0\omega_{j'}}\begin{pmatrix} & \mathrm{Re}\left(\Big[(\mathcal{H}\mathbf{e}_j\cdot\mathcal{H}\mathbf{e}_{j'})k_{z,j'}-(\mathcal{H}\mathbf{e}_j\cdot\mathbf{k}_{j'})e_{z,j'}\Big]e^{i(k_{z,j}+k_{z,j'})z_0}\,\mathrm{sinc}\left(\frac{\ell(\boldsymbol{\kappa}_j+\boldsymbol{\kappa}_{j'})}{2\pi}\right)\right) \\ + & \mathrm{Re}\left(\Big[(\mathcal{H}\mathbf{e}^*_j\cdot\mathcal{H}\mathbf{e}_{j'})k_{z,j'}-(\mathcal{H}\mathbf{e}^*_j\cdot\mathbf{k}_{j'})e_{z,j'}\Big]e^{-i(k_{z,j}-k_{z,j'})z_0}\,\mathrm{sinc}\left(\frac{l(\boldsymbol{\kappa}_j-\boldsymbol{\kappa}_{j'})}{2\pi}\right)\right)\end{pmatrix}} \tag{4.38}$$

5. MICROGRID IMAGING EQUATION

Now each pixel can be modeled as located on a grid at $(m\ell, n\ell)$ then plugging in rect $\left(\frac{x-m\ell}{\ell}, \frac{y-n\ell}{\ell}\right)$ for rect $\left(\frac{x}{\ell}, \frac{y}{\ell}\right)$ into the derivation of equation 4.38 and taking $z_0 \to 0$ yields:

$$
\begin{aligned}
&[\mathbf{g}]_{m,n} = \\
&\sum_j \sum_{j'} \frac{\ell^2}{\mu_0 \omega_{j'}} \left(\begin{array}{rl} & \mathrm{Re}\left(\left[(\mathcal{H}\mathbf{e}_j \cdot \mathcal{H}\mathbf{e}_{j'}) k_{z,j'} - (\mathcal{H}\mathbf{e}_j \cdot \mathbf{k}_{j'}) e_{z,j'} \right] e^{i(k_{z,j}+k_{z,j'})z_0} e^{i\boldsymbol{\ell}_{m,n}\cdot\boldsymbol{\kappa}_{j'}} \operatorname{sinc}\left(\frac{\ell(\boldsymbol{\kappa}_j+\boldsymbol{\kappa}_{j'})}{2\pi} \right) \right) \\ + & \mathrm{Re}\left(\left[(\mathcal{H}\mathbf{e}_j^* \cdot \mathcal{H}\mathbf{e}_{j'}) k_{z,j'} - (\mathcal{H}\mathbf{e}_j^* \cdot \mathbf{k}_{j'}) e_{z,j'} \right] e^{-i(k_{z,j}-k_{z,j'})z_0} e^{-i\boldsymbol{\ell}_{m,n}\cdot\boldsymbol{\kappa}_{j'}} \operatorname{sinc}\left(\frac{l(\boldsymbol{\kappa}_j-\boldsymbol{\kappa}_{j'})}{2\pi} \right) \right) \end{array} \right)
\end{aligned}
\tag{5.1}
$$

where the vector $\boldsymbol{\ell}_{m,n} = (m\ell, n\ell)$, $\theta_{m,n}$ is the orientation of the polarizer at pixel (m, n). The z-component of $\mathbf{f}$, f_z and the terms multiplied by it cancel out in the above equation for any $\mathcal{H}$ or $\mathcal{H}^2$. The result is that any z-component of the original $\mathbf{f}$ is in the null space.

6. CONCLUSIONS

Microgrid polarimeters have a lot of potential now that lithography techniques facilitate manufacturing wire grid polarizers for the visible spectrum. Microgrid polarimeters have the advantages of having broad spectral bandwidth, large angles of acceptance, and ease of calibration.

I have derived the (ideal) imaging operator for a microgrid polarimeter, and it appears to be different from the Stokes formalism equivalent (this needs to be proven however). The operator elucidates the physical phenomena inherent in a microgrid array, and provides a path to a theoretically sound inversion operator for the estimation of the original field.

Future work includes comparing the operator derived in this paper with the traditional Stokes formalism, inverting the operator, and inverting the operator in the presence of noise.

REFERENCES

[1] Cheng, L. J., Hamilton, M., Mahoney, C., and Reyes, G., "Analysis of aotf hyperspectral imaging," in [*Algorithms for Multispectral and Hyperspectral Imagery*], Iverson, A., ed., *Proc. SPIE* **2231**, 15816 (1994).

[2] Tyo, J. S., Rowe, M. P., E. N. Pugh, J., and Engheta, N., "Target detection in optically scattering media by polarization-difference imaging," *Appl. Opt.* **35**, 1855–1870 (Apr 1996).

[3] Schechner, Y. Y., Narasimhan, S. G., and Nayar, S. K., "Polarization-based vision through haze," in [*ACM SIGGRAPH ASIA 2008 courses*], *SIGGRAPH Asia '08*, 71:1–71:15, ACM, New York, NY, USA (2008).

[4] Silverman, M. P. and Strange, W., "Object delineation within turbid media by backscattering of phase-modulated light," *Optics Communications* **144**(1-3), 7 – 11 (1997).

[5] Thilak, V., Voelz, D. G., and Creusere, C. D., "Image segmentation from multi-look passive polarimetric imagery," *Polarization Science and Remote Sensing III* **6682**(1), 668206, SPIE (2007).

[6] Diner, D. J., Davis, A., Hancock, B., Gutt, G., Chipman, R. A., and Cairns, B., "Dual-photoelastic-modulator-based polarimetric imaging concept for aerosol remote sensing," *Appl. Opt.* **46**, 8428–8445 (Dec 2007).

[7] Sassen, K., "Polarization in Lidar," in [*Lidar*], Weitkamp, C., ed., *Springer Series in Optical Sciences* **102**, 19–42, Springer Berlin / Heidelberg (2005).

[8] Tyler, D. W., Phenis, A. M., Tietjen, A. B., Virgen, M., Mudge, J. D., Stryjewski, J. S., and Dank, J. A., "First high-resolution passive polarimetric images of boosting rocket exhaust plumes," *Polarization Science and Remote Sensing IV* **7461**(1), 74610J, SPIE (2009).

[9] Dymond, J. R. and Shepherd, J. D., "Correction of the topographic effect in remote sensing," *IEEE Transactions on Geoscience and Remote Sensing* **37**, 2618–2619 (Sept. 1999).

[10] Treuhaft, R. N. and Cloude, S. R., "The structure of oriented vegetation from polarimetric interferometry," *IEEE Transactions on Geoscience and Remote Sensing* **37**, 2620–2624 (Sept. 1999).

[11] Blakeney, S. L., Day, S. E., and Stewart, J. N., "Determination of unknown input polarisation using a twisted nematic liquid crystal display with fixed components," *Optics Communications* **214**(1-6), 1 – 8 (2002).

[12] Wolfe, J. E. and Chipman, R. A., "Polarimetric characterization of liquid-crystal-on-silicon panels," *Appl. Opt.* **45**, 1688–1703 (Mar 2006).

[13] Bowers, D. L., Boger, J. K., Wellems, L. D., Ortega, S. E., Fetrow, M. P., Hubbs, J. E., Black, W. T., Ratliff, B. M., and Tyo, J. S., "Unpolarized calibration and nonuniformity correction for long-wave infrared microgrid imaging polarimeters," *Optical Engineering* **47**(4), 046403 (2008).

[14] Ratliff, B. M., Boger, J. K., Fetrow, M. P., Tyo, J. S., and Black, W. T., "Image processing methods to compensate for IFOV errors in microgrid imaging polarimeters," *Polarization: Measurement, Analysis, and Remote Sensing VII* **6240**(1), 62400E, SPIE (2006).

[15] Ratliff, B. M., LaCasse, C. F., and Tyo, J. S., "Interpolation strategies for reducing IFOV artifacts in microgrid polarimeter imagery," *Opt. Express* **17**, 9112–9125 (May 2009).

[16] Ratliff, B. M., Tyo, J. S., Boger, J. K., Black, W. T., Bowers, D. L., and Fetrow, M. P., "Dead pixel replacement in LWIR microgrid polarimeters," *Opt. Express* **15**, 7596–7609 (Jun 2007).

[17] Tyo, J. S., LaCasse, C. F., and Ratliff, B. M., "Total elimination of sampling errors in polarization imagery obtained with integrated microgrid polarimeters," *Opt. Lett.* **34**, 3187–3189 (Oct 2009).

[18] LaCasse, C. F., Chipman, R. A., and Tyo, J. S., "Band limited data reconstruction in modulated polarimeters," *Opt. Express* **19**, 14976–14989 (Aug 2011).

[19] Wolfe, J. and Chipman, R., "Reducing symmetric polarization aberrations in a lens by annealing," *Opt. Express* **12**, 3443–3451 (Jul 2004).

[20] Barrett, H. H. and Myers, K. J., [*Foundations of Image Science*], Wiley-Interscience, Hoboken, New Jersey, United States (2004).

[21] Gaskill, J. D., [*Linear Systems, Fourier Transforms, and Optics*], Wiley Series in Pure and Applied Mathematics, New York, Chichester, Brisbane, Toronto (1978).

[22] Goodman, J. W., [*Introduction to Fourier Optics*], McGraw-Hill, New York, St. Louis, Toronto, London, Sydney (1968).

[23] Yu, X. J. and Kwok, H. S., "Optical wire-grid polarizers at oblique angles of incidence," *Journal of Applied Physics* **93**(8), 4407–4412 (2003).

[24] Born, M. and Wolf, E., [*Principles of Optics*], Cambridge University Press, New York, Cambridge, Madrid, Port Melbourne (2003).

[25] Hansen, D., Gardner, E., Perkins, R., Lines, M., and Robbins, A., "Invited paper: The display applications and physics of the ProFlux™wire grid polarizer," *SID'02* (9), 730–733 (2002).

[26] Wolf, E., [*Introduction to the Theory of Coherence and the Polarization of Light*], Cambridge University Press, New York, United States (2007).

[27] Goldstein, D., [*Polarized Light*], Marcel Dekker, New York, Basel (2003).

[28] Tyo, J. S., "Design of optimal polarimeters: maximization of signal-to-noise ratio and minimization of systematic error," *Applied Optics* **41 (4)**, 619–630 (2002).

[29] Kay, S. M., [*Fundamentals of Statistical Signal Processing : Estimation Theory*], Prentice Hall PTR, Upper Saddle River, New Jersey, United States (1993).

[30] Lax, P. D., [*Functional Analysis*], Wiley-Interscience, New York, New York (2002).